

# Activation cross-sections of longer lived radioisotopes of deuteron induced nuclear reactions on terbium up to 50 MeV

F. Tárkányi<sup>a</sup>, S. Takács<sup>a</sup>, F. Ditrói<sup>a,\*</sup>, A. Hermanne<sup>b</sup>, A.V. Ignatyuk<sup>c</sup>

<sup>a</sup>*Institute of Nuclear Research of the Hungarian Academy of Sciences (ATOMKI), Debrecen, Hungary*

<sup>b</sup>*Cyclotron Laboratory, Vrije Universiteit Brussel (VUB), Brussels, Belgium*

<sup>c</sup>*Institute of Physics and Power Engineering (IPPE), Obninsk, Russia*

## Abstract

Experimental cross-sections are presented for the first time for the  $^{159}\text{Tb}(d,xn)^{155,157,159}\text{Dy}$ ,  $^{155,156,160}\text{Tb}$  and  $^{153}\text{Gd}$  nuclear reactions up to 50 MeV. The experimental data are compared with theoretical predictions of the ALICE, EMPIRE and TALYS nuclear reaction codes. Integral thick-target yields are also derived for the reaction products that have practical applications.

*Keywords:* terbium target, stacked foil technique, terbium, dysprosium and gadolinium radioisotopes, theoretical model codes, physical yield

## 1. Introduction

The aim of the work was manifold:

- Very few experimental data exist in the literature for lanthanides, both for proton and deuteron induced reactions.
- The quality of the database for activation cross-sections of deuteron induced reactions is poor, compared to what exists for proton induced reaction. In our laboratories a systematic study of the activation cross-sections of deuteron induced reactions for different applications is in progress up to 50 MeV [1, 2].
- Several radionuclides of the lanthanide group are becoming increasingly important in the field of nuclear medicine (diagnostic and therapeutic radioisotopes) [3–5].
- The prediction capability of the nuclear reaction model codes is still limited in case of deuteron induced reactions. Further improvement requires comparisons with experimental data. As terbium is monoisotopic, the targetry is simpler and cheaper and the cross-section results for a given activation product are not infected by contributions of multiple processes on the different stable target isotopes,

hence no need for use of enriched target technology.

- Activation cross-sections on Tb are required for production of the medically related  $^{159}\text{Dy}$  [6] and  $^{157}\text{Dy}$  [7–9] and need to be compared with other possible production routes.

In a literature search only two experimental cross-sections data sets were found, published by Duc et al. [10] for production of  $^{159}\text{Dy}$ ,  $^{157}\text{Dy}$  and  $^{160}\text{Tb}$  up to 27 MeV and by Siri et al. [11] for production of  $^{157}\text{Dy}$  and  $^{160}\text{Tb}$  up to 27 MeV. Mukhammedov et al. [12] measured integral yields of  $^{159}\text{Dy}$  as a function of the deuteron energy up to 12 MeV for charged particle activation analysis.

## 2. Experimental and data evaluation

The general characteristics and procedures for irradiation, activity assessment and data evaluation (including estimation of uncertainties) were similar to what is discussed in several earlier works of our group [13, 14]. The main experimental parameters for the present study are summarized in Table 1. The principal methods used in data evaluation and the used decay data are collected in Table 2 [13, 15–22] and in Table 3. The good overlap of the re-measured excitation function for the  $^{27}\text{Al}(d,xn)^{24}\text{Na}$  monitor reaction with the recommended values [23] is illustrated in Fig. 1.

\*Corresponding author: ditroi@atomki.hu

Table 3: Investigated radionuclides, their decay properties and production routes

Nuclide decay mode	Half-life	$E_{\gamma}$ (keV)	$I_{\gamma}$ (%)	Contributing reaction	Q-value (keV)
$^{159}\text{Dy}$ $\epsilon$ : 100 %	144.4 d	58.0	2.27	$^{159}\text{Tb}(d,2n)$	-3372.48
$^{157}\text{Dy}$ $\epsilon$ : 100 %	8.14 h	182.424 326.336	1.33 93	$^{159}\text{Tb}(d,4n)$	-19260.72
$^{155}\text{Dy}$ $\epsilon$ : 100 %	9.9 h	184.564 226.918	3.37 % 68.4	$^{159}\text{Tb}(d,6n)$	-35671.3
$^{153}\text{Dy}$ $\alpha$ : 0.0094 $\epsilon$ : 99.9906	6.4 h	80.723 99.659 213.754 254.259 274.673 389.531 537.225 1023.99	11.1 10.51 10.9 8.6 3.1 1.52 1.33 1.09	$^{159}\text{Tb}(d,8n)$	-51824.12
$^{160}\text{Tb}$ $\beta^-$ : 100 %	72.3 d	86.7877 197.0341 215.6452 298.57 83 879.378 962.311 966.166 1177.954	13.2 5.18 4.02 26.1 30.1 9.81 25.1 14.9	$^{159}\text{Tb}(d,p)$	4150.644
$^{156}\text{Tb}$ $\epsilon$ : 100 %	5.35 d	88.97 199.19 262.54 296.49 356.38 422.34 534.29 1065.11 1154.07 1159.03 1222.44 1421.67	18 41 5.8 4.5 13.6 8.0 67 10.8 10.4 7.2 31 12.2	$^{159}\text{Tb}(d,p4n)$	-25880.05
$^{155}\text{Tb}$ $\epsilon$ : 100 %	5.32 d	86.55 105.318 148.64 161.29 163.28 180.08 340.67 367.36	32.0 25.1 2.65 2.76 4.44 7.5 1.18 1.48	$^{159}\text{Tb}(d,p5n)$ $^{153}\text{Dy}$ decay	-32794.5
$^{153}\text{Gd}$ $\epsilon$ : 100 %	240.4 d	97.43100 103.18012	29.0 21.1	$^{159}\text{Tb}(d,2p6n)$ $^{153}\text{Dy}$ decay	-46519.36

When complex particles are emitted instead of individual protons and neutrons the Q-values have to be decreased by the respective binding energies of the compound particles: np-d, +2.2 MeV; 2np-t, +8.48 MeV; n2p- $^3\text{He}$ , +7.72 MeV; 2n2p- $\alpha$ , +28.30 MeV

### 3. Theoretical calculations

We compared our measured cross-sections with predictions of the ALICE-IPPE [24], EMPIRE [25] and TALYS [26] nuclear reaction codes. The TALYS results were taken from the TENDL 2011 and TENDL 2012 nuclear reaction libraries [27]. We present both versions to show the improvements and the still remaining problems between the two versions of the code. In case of ALICE and EMPIRE we have used the codes modified for better description of deuteron induced reactions (EMPIRE-D and ALICE-IPPE D) described in more detail in our previous reports [28, 29].

### 4. Results and discussion

#### 4.1. Excitation functions

The measured cross-sections for the production of the activation products are presented in Table 4 and Figs.

2-8. All cross-section values of dysprosium radionuclides are due to direct production via (d,xn) reactions. The terbium radioproducts are produced only directly via (d,pxn) reactions or additionally through the decay of the shorter-lived isobaric parent dysprosium radioisotope (cum). The investigated  $^{153}\text{Gd}$  is produced directly via (d,2pxn) reaction (including complex particle emission) and from the decay of parent  $^{153}\text{Tb}$  radioisotope. The ground state of the produced radioisotopes above the direct production can be produced additionally through the internal transition of the isomeric state. The cross-section is marked with (m+) when the half-life of the isomeric state is significantly shorter comparing to the half-life of the ground state and the cross-sections of the production of ground state were deduced from spectra after nearly complete decay of the isomeric state.

Table 1: Main experimental parameters for 2 irradiation sessions

Reaction	$^{159}\text{Tb}(d,x)$	$^{159}\text{Tb}(d,x)$
Incident particle	Deuteron	Deuteron
Method	Stacked foil	Stacked foil
Target and thickness	Tb foil, 95.47 $\mu\text{m}$	Tb foil, 95.47 $\mu\text{m}$
Number of Tb target foils	15	7
Target composition	Tb, Dy, Al	Tb, Eu, Sb, Pb, Al
Accelerator	Cyclone 90 cyclotron of the Universit Catholique in Louvain la Neuve (LLN)	Cyclone 90 cyclotron of the Universit Catholique in Louvain la Neuve (LLN)
Primary energy	50 MeV	50 MeV
Covered energy range	49.6-7.9	48.5-36.1
Irradiation time	60 min	93 min
Beam current	104.94 nA	103.46 nA
Monitor reaction [23]	$^{27}\text{Al}(d,x)^{24}\text{Na}$ reaction	$^{27}\text{Al}(d,x)^{24}\text{Na}$ reaction
Monitor target and thickness	$^{nat}\text{Al}$ , 26.76 $\mu\text{m}$	$^{nat}\text{Al}$ , 49.06 $\mu\text{m}$
detector	HpGe	HpGe
$\gamma$ -spectra measurements	4 series	4 series
Cooling times after EOB	4.3-7.3 h, 49.8-69.5 h, 581.7-652.5 h 2277.0-2422.8 h	7.0-8.3 h, 45.1-47.2 h 256.6-364.4 h, 2373.3-2432.4 h

Table 2: Main parameters of data evaluation (with references)

Gamma spectra evaluation	Genie 2000, Forgamma	[? ]
Determination of beam intensity	Faraday cup (preliminary) Fitted monitor reaction (final)	[17]
Decay data	NUDAT 2.6	[18]
Reaction Q-values	Q-value calculator	[19]
Determination of beam energy	CityplaceAnderson (preliminary) Fitted monitor reaction (final)	[20] [13]
Uncertainty of energy	Cumulative effects of possible uncertainties	
Cross-sections	Reaction cross-section on element and on single isotope	
Uncertainty of cross-sections	Sum in quadrature of all individual linear contributions	[21]
Yield	Physical yield	[22]

#### 4.1.1. Production of $^{159}\text{Dy}$ ( $T_{1/2}=144.4$ d)

According to Fig. 2 our data are systematically higher than the earlier results of Duc et al. [10]. The agreement with the results of the theoretical codes is acceptable, not counting the generally observed underestimation of the high energy cross-sections by the theory.

#### 4.1.2. Production of $^{157}\text{Dy}$ ( $T_{1/2}=8.14$ h)

The present and the earlier experimental data for the  $^{159}\text{Tb}(d,4n)^{157}\text{Dy}$  reaction are shown in Fig. 3. The agreement between all experimental data is acceptable. No explanation for the second bump around 50 MeV predicted by TENDL 2011 and 2012 was found. For comparison of the productions routes the cross-sections of Lebowitz et al. [7] for the  $^{159}\text{Tb}(p,3n)$  reaction are also shown.

#### 4.1.3. Production of $^{155}\text{Dy}$ ( $T_{1/2}=9.9$ h)

No earlier experimental data were found in the literature. Comparison with the theory in the overlapping energy range shows a good agreement for EMPIRE-D, while the two other codes overestimate by a factor of 2

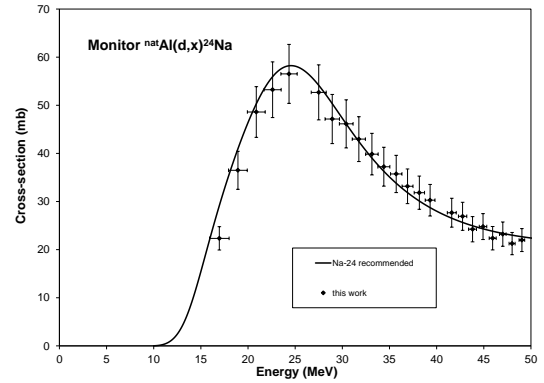


Figure 1: The simultaneously measured monitor reactions for determination of deuteron beam energy and intensity

to 5 at 50 MeV (Fig. 4). No explanations, however for the second bump around 90 MeV predicted by TENDL 2011 and 2012.

#### 4.1.4. Production of $^{160}\text{Tb}$ ( $T_{1/2}=72.3$ d)

We have only a few experimental data points at low energies around the maximum of the excitation function (Fig. 5). Our experimental data are significantly higher than the experimental data of Duc et al [10] and a little lower compared to the data of Siri et al. [11]. The theoretical predictions of the two TENDL libraries are a factor of two low, compared to the experimental data, while EMPIRE-D and ALICE-D reproduce rather well the shape and values of our experiment.

#### 4.1.5. Production of $^{156}\text{Tb}$ ( $T_{1/2}=5.35$ d) (m+)

The  $^{156}\text{Tb}$  is produced only directly via (d,p4n) reaction. The  $^{156}\text{Tb}$  has a long-lived ground state ( $T_{1/2}=5.35$  d) and two shorter-lived isomeric states (5.3 h and 24.4 h) decaying completely to the ground state. Our experimental data for production of ground state (Fig. 6) were deduced from spectra after nearly complete decay of the isomeric states (m+). No earlier experimental data exist for comparison. The data in TENDL libraries show that the ground state is produced mostly directly. The contribution from the isomeric decay is small. In the overlapping energy range the theoretical data slightly overestimate the experimental results.

#### 4.1.6. Production of $^{155}\text{Tb}$ ( $T_{1/2}=5.32$ d) (cum)

The measured experimental data (Fig. 7) are cumulative and are the sum of direct production and total de-

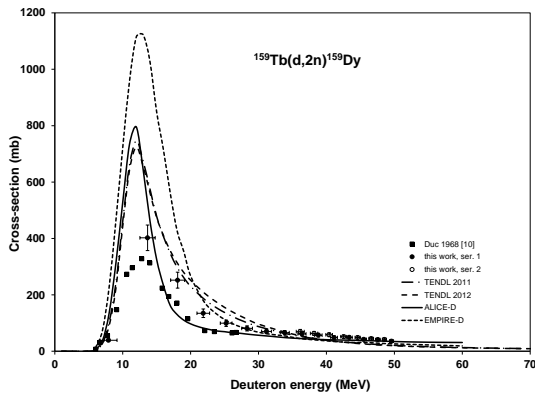


Figure 2: Experimental and theoretical excitation functions of the  $^{159}\text{Tb}(d,2n)^{159}\text{Dy}$  reaction

cay of the shorter lived  $^{155}\text{Dy}$  (9.9 h) parent radioisotope. By referring to the excitation function of the  $^{155}\text{Dy}$  (Fig. 4) the main contributor to the cumulative cross-section of  $^{155}\text{Tb}$  is the decay of the parent  $^{155}\text{Dy}$ . This is confirmed by the results in the TENDL libraries. The best result is given by the EMPIRE-D model calculation, while ALICE-D and TENDL results overestimate the experimental values for the cumulative case.

#### 4.1.7. Production of $^{153}\text{Gd}$ ( $T_{1/2}=240.4$ d) (cum)

The experimental data for cumulative production of the  $^{153}\text{Gd}$  are shown in Fig. 8. The experimental data were deduced from spectra measured after decay of the parent decay chain ( $^{153}\text{Dy}$  6.4 h,  $^{153}\text{Tb}$  2.34 d). No earlier experimental data are available. The theoretical calculations display a rather large spread of the corresponding yields. For all codes the main contributions below 60 MeV are connected with the  $\alpha$ -particle emission channels and the additional increases of the production cross-sections above 60 MeV are produced by the cumulative channels related to the decay of predecessors. TENDL-2012 underestimates distinctly the direct production of  $^{153}\text{Gd}$ , while ALICE-D and EMPIRE-D strongly overestimate it. The obtained differences of the code results are the consequence of models used for a simulation of the  $\alpha$ -particle emission.

#### 4.2. Integral yields

The so called physical integral yield (instantaneous short irradiation) [22] as a function of the incident deuteron energy was calculated from a spline fit to our experimental data and are shown in Fig. 9 and Fig.

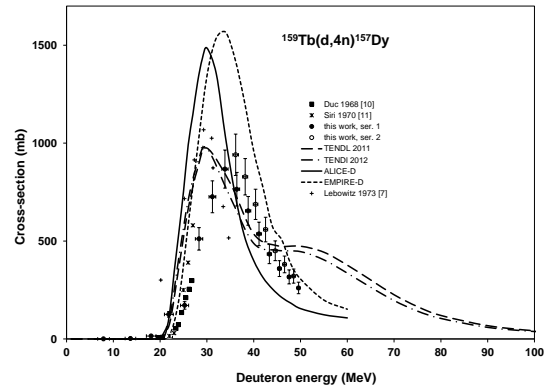


Figure 3: Experimental and theoretical excitation functions of the  $^{159}\text{Tb}(d,4n)^{157}\text{Dy}$  reaction

10. The only measurement find in the literature is from Mukhamedov [12] for  $^{160}\text{Tb}$  and  $^{159}\text{Dy}$ . Our data are significantly higher than those given by Mukhamedov for both referred radioisotopes.

### 5. Comparison of the experimental and theoretical results

The comparison with the results of theoretical codes using global parameters shows that still large difference can be observed between the experimental results and the predictions the different codes. The new improvements for better description of the complex deuteron induced reactions resulted in a better description. The predictions for (d,pxn) reactions by of ALICE-D and EMPIRE-D are naturally the most successful, as the correction included is based more directly on the systematics of experimental data. The agreement with the 2012 TENDL version is better, but the (d,p) reaction is still strongly under-predicted.

### 6. Comparison of the production routes of $^{157}\text{Dy}$ and $^{159}\text{Dy}$

Among the investigated reactions the routes leading to production of  $^{157}\text{Dy}$  and  $^{159}\text{Dy}$  have presently a practical interest. The two radioisotopes can be produced via various reactions. Out of these competitive production routes we discuss below the low energy, light charged particle methods in more detail, while summarizing briefly the other routes.

Table 4: Measured cross-sections of the  $^{159}\text{Tb}(d,x)^{159,157,155}\text{Dy}$ ,  $^{159}\text{Tb}(d,x)^{160,156g,155}\text{Tb}$  and  $^{159}\text{Tb}(d,x)^{153}\text{Gd}$  reactions

E $\pm$ $\Delta$ E (MeV)	Cross-section $\sigma \pm \Delta\sigma$ (mb)																
	$^{159}\text{Dy}$			$^{157}\text{Dy}$			$^{155}\text{Dy}$		$^{160}\text{Tb}$			$^{156g}\text{Tb}$		$^{153}\text{Tb}$		$^{153}\text{Gd}$	
3.3	1.3	39.1	4.5	0.5	0.1			48.8	5.5	0.4	0.0						
11.0	1.2	402.3	45.2	2.3	0.3			196.5	22.1	0.4	0.1						
16.0	1.1	252.1	28.4	15.0	1.7			126.7	14.2	0.5	0.1						
20.0	1.0	134.8	15.2	125.6	14.1			100.4	11.3	0.5	0.1						
23.6	0.9	99.4	11.2	171.4	19.2			74.9	8.4	0.6	0.1						
26.8	0.8	81.0	9.2	511.2	57.4			69.2	7.8	0.6	0.1						
29.8	0.7	70.3	7.9	726.0	81.5			56.3	6.3	1.6	0.2						
32.5	0.7	65.9	7.6	867.4	97.4			55.3	6.2	3.1	0.4						
35.1	0.6	61.5	6.9	764.6	85.8			47.3	5.3	5.1	0.6						
36.1	0.6	69.6	7.8	940.5	105.6												
37.6	0.6	57.0	6.5	654.2	73.4			44.4	5.0	9.3	1.1	0.4	0.1	0.3	0.1		
38.2	0.5	63.2	7.1	828.0	93.0												
40.0	0.5	48.7	5.6	536.4	60.2	1.0	0.1	41.2	4.6	17.6	2.0	2.0	0.2	1.6	0.2		
40.4	0.5	58.6	6.6	687.5	77.2												
42.3	0.4	49.2	5.6	433.6	48.7	10.9	1.2	37.3	4.2	32.2	3.6	12.5	1.4	4.3	0.5		
42.5	0.4	51.7	5.8	558.8	62.7	2.2	0.3										
44.4	0.4	42.0	4.8	359.4	40.3	21.1	2.4	34.8	3.9	47.4	5.3	40.9	4.5	7.7	0.9		
44.6	0.4	48.6	5.5	450.2	50.5	20.8	2.3										
46.5	0.3	41.5	4.7	317.0	35.6	70.2	7.9	33.2	3.7	65.5	7.4	93.6	10.3	11.3	1.3		
46.6	0.3	44.8	5.1	380.8	42.8	86.5	9.7										
48.5	0.3	41.8	4.8	321.0	36.0	97.8	11.0										
48.6	0.3	35.8	4.1	260.6	29.2	177.0	19.9	31.9	3.6	74.5	8.4	195.5	21.3	15.4	1.7		

Table 5: Production routes of  $^{159}\text{Dy}$  and  $^{157}\text{Dy}$

$^{159}\text{Dy}$			$^{157}\text{Dy}$		
Reaction	Energy range	Ref	Reaction	Energy range	Reference
$^{159}\text{Tb}(p,n)$	25-6	[8, 30]	$^{159}\text{Tb}(p,3n)$	30-20	[7]
$^{159}\text{Tb}(d,2n)$	20-10	[7, 10], this work	$^{159}\text{Tb}(d,4n)$	50-25	[11], this work
$^{150}\text{Gd}(\alpha,n)$	25-15	TENDL	$^{154}\text{Gd}(\alpha,n)$	25-15	TENDL
$^{157}\text{Gd}(\alpha,2n)$	30-18	TENDL	$^{155}\text{Gd}(\alpha,2n)$	30-20	TENDL
$^{nat}\text{Gd}(\alpha,xn)$	50-20	TENDL	$^{155}\text{Gd}(\alpha,He,n)$	30-15	TENDL
$^{157}\text{Gd}(\alpha,He,n)$	30-15	TENDL	$^{156}\text{Gd}(\alpha,He,2n)$	50-20	TENDL
$^{158}\text{Gd}(\alpha,He,2n)$	40-18	TENDL			
$^{nat}\text{Gd}(\alpha,He,xn)$	50-20	TENDL			

The  $^{157}\text{Dy}$  and  $^{159}\text{Dy}$  can be produced with the following bombarding beams and nuclear reactions:

- By neutron induced reactions via  $(n,\gamma)$  on the neighboring stable Dy isotopes. The production yield is high. It requires highly enriched Dy targets to have radionuclidic pure end-products. The product is of low specific activity and is not carrier free [31].
- By photonuclear reactions [32]. The product has usually low specific activity by using  $(\gamma,xn)$  at the presently used intensities and it is not carrier free. The specific activity could be significantly increased by using the new high intensity  $\gamma$ -beams.
- By high energy spallation reaction and use of electromagnetic separators [33]. The method assures a high specific activity, but the yield is low and the product will be expensive. It can be used in cases when no other method is available. Mostly in case of exotic and uncommon radioisotopes.
- By low and medium energy light charged particle

induced nuclear reactions. The production yield is acceptable high. In favorable cases production does not require highly enriched targets. The end product is mostly carrier free and has high specific activity.

For routine production, reactor production is often the most favorable, if the radionuclide fulfills the requirement of the applications (specific activity). Many medically interesting radionuclides can, however, be produced only with charged particle beams. The low and medium energy, high power (beams up to 1 mA) cyclotrons are also becoming more competitive for production of those radioisotopes, which presently produced in nuclear reactors. Photonuclear and spallation based methods are still not common, these methods need improvements on the beam intensity. The main production routes for  $^{157}\text{Dy}$  and  $^{159}\text{Dy}$  via light charged particle beam are summarized in Table 5 [7, 8, 10, 11, 30]. The excitation functions of the reactions are shown in Fig. 11 and 12.

Taking into account that for many of the involved excitation function no experimental data exist, the excita-

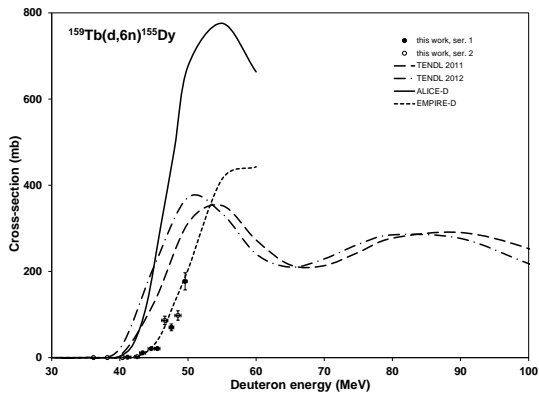


Figure 4: Experimental and theoretical excitation functions of the  $^{159}\text{Tb}(d,6n)^{155}\text{Dy}$  reaction

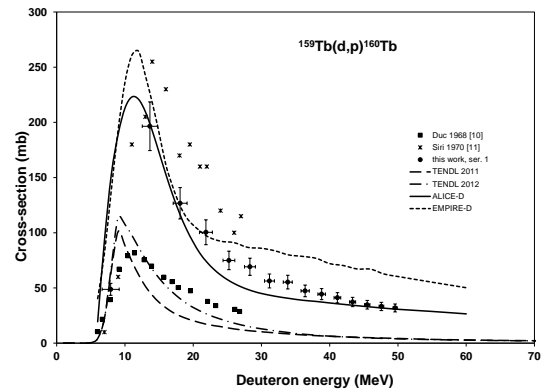


Figure 5: Experimental and theoretical excitation functions of the  $^{159}\text{Tb}(d,p)^{160}\text{Tb}$  reaction

tion functions are based on the adjusted theoretical predictions of the TENDL 2012 library. The differences in the different routes are so high that conclusion is not affected by the known poor prediction capability of the theoretical results.

### 6.1. Production routes of $^{159}\text{Dy}$

According to Table 5 and Fig. 11 the most favorable route for production of  $^{159}\text{Dy}$  at a low energy cyclotron ( $k = 20$ ) is the  $^{159}\text{Tb}(p,n)$  process and at higher energies ( $k = 35$ ) the  $^{159}\text{Tb}(d,2n)$  reaction. The yield of the  $(d,2n)$  reaction is, like in many cases we discussed earlier, significantly higher than the yield of  $(p,n)$ . According to Fig. 11 the cross-sections of the  $^3\text{He}$  induced reactions are very small, similar to cross-sections of the  $(\alpha,n)$  reaction. The  $(\alpha,2n)$  process requires a 30 MeV cyclotron and highly enriched target. The cross-section is high but has lower yield comparing to the  $(d,2n)$  reaction due to the shorter range of the alpha particle. The  $^{159}\text{Dy}$  can also be produced with high radionuclide purity on  $^{nat}\text{Gd}$  by both  $(^3\text{He},xn)$  and alpha particle induced reactions. In both cases the yield is low.

### 6.2. Production routes of $^{157}\text{Dy}$

According to the Fig. 12 at a low energy cyclotron only the low yield  $^{154}\text{Gd}(\alpha,n)$  reaction is available. At commercial 30-35 MeV  $\text{H}^-$ -cyclotrons the  $^{159}\text{Tb}(p,3n)$  reaction results in high production yields. In the optimum (30-20 MeV) energy range the amount of the simultaneously produced  $^{159}\text{Dy}$  is small due to the low cross-sections of the  $(p,n)$  in this higher energy range

(see Fig. 12). The energy range for the  $(d,4n)$  reaction should be 50-30 MeV to minimize the amount of  $^{159}\text{Dy}$  produced simultaneously via  $(d,2n)$ . Accelerators capable of practical implementation of the  $(d,4n)$  reaction are however very rare. The  $^{155}\text{Gd}(\alpha,2n)$  requires highly enriched targets and cyclotrons with 30 MeV alpha beams, and the yield is significantly lower compared to the  $^{159}\text{Tb}(p,3n)$  reaction. To get high radionuclide purity highly enriched  $^{155}\text{Gd}$  and  $^{156}\text{Gd}$  targets should be used in case of  $^3\text{He}$ -particle induced reactions. The yield however is very low and the  $^3\text{He}$  beam is expensive even having recovery system for the gas in the ion source.

## 7. Summary and conclusion

The present work provides new data for the excitation function of deuteron induced nuclear reactions on natural terbium, which is actually  $^{159}\text{Tb}$ . The experimental results for the produced radioisotopes were compared with the former literature values as well as with the results of theoretical model calculations by using the codes ALICE-D, EMPIRE-D and TALYS 1.4 (the data taken from the TENDL 2011 and 2012 libraries). Our new measurements both verified or improved the former results and gave an extension to them. Comparison with the results of model codes could validate the recent improvements of those, as well as provide new basis for further improvements. As practical results, physical yield curves were also calculated for medical and other practical use. Serving for the present demands of radioisotopes research a detailed comparison is given

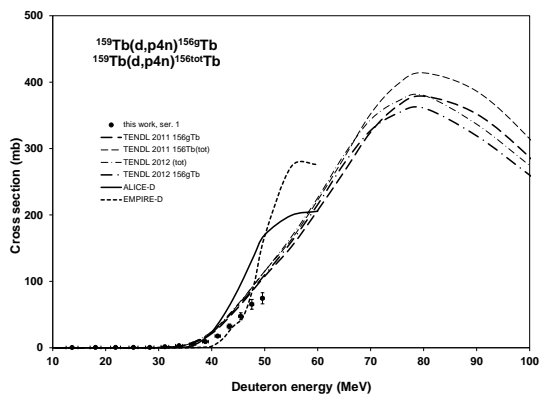


Figure 6: Experimental and theoretical excitation functions of the  $^{159}\text{Tb}(d,p4n)^{156g}\text{Tb}(m+)$  reaction

for the possible routes for production of 2 important radioisotopes  $^{157}\text{Dy}$  and  $^{159}\text{Dy}$ .

## 8. Acknowledgements

This study was partly performed in the frame of the MTA-FWO (Vlaanderen) collaboration programs. The authors thank the different research projects and their respective institutions for the practical help and providing the use of the facilities for this study.

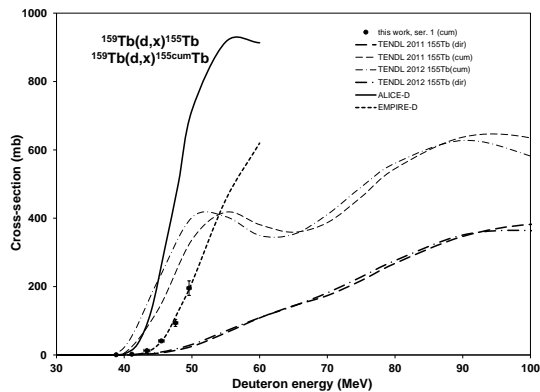


Figure 7: Experimental and theoretical excitation functions of the  $^{159}\text{Tb}(d,x)^{155}\text{Tb}(\text{cum})$  reaction

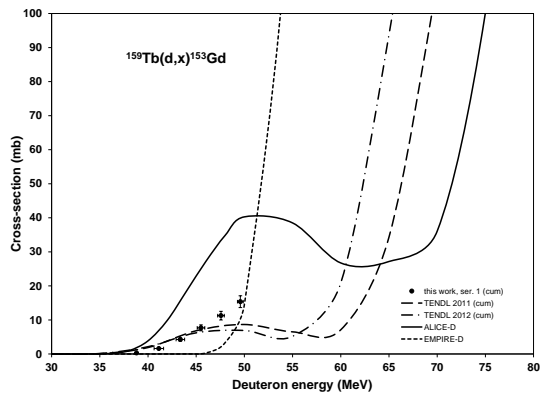


Figure 8: Experimental and theoretical excitation functions of the  $^{159}\text{Tb}(d,x)^{153}\text{Gd}(\text{cum})$  reaction

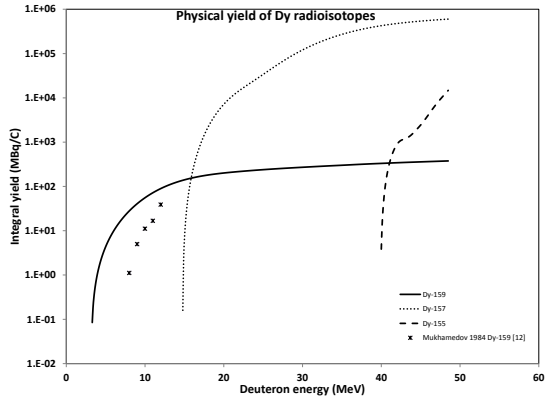


Figure 9: Thick target yields for radionuclides of dysprosium produced by deuteron irradiation on  $^{159}\text{Tb}$  and comparison with the available literature values

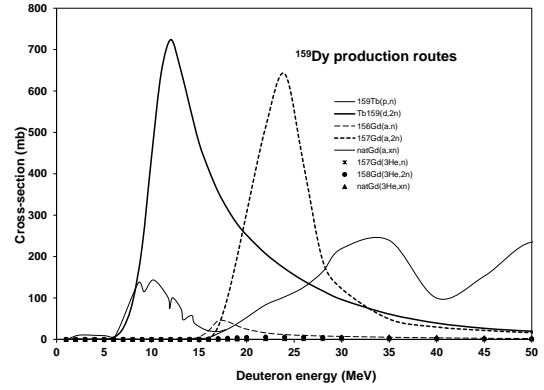


Figure 11: Comparison of excitation functions for production of  $^{159}\text{Dy}$

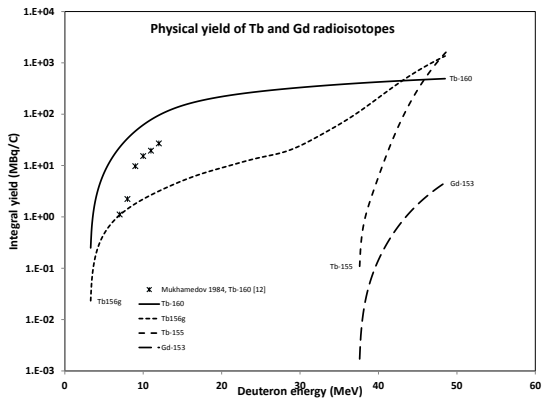


Figure 10: Thick target yields for radionuclides of terbium and gadolinium produced by deuteron irradiation on  $^{159}\text{Tb}$  and comparison with the available literature values

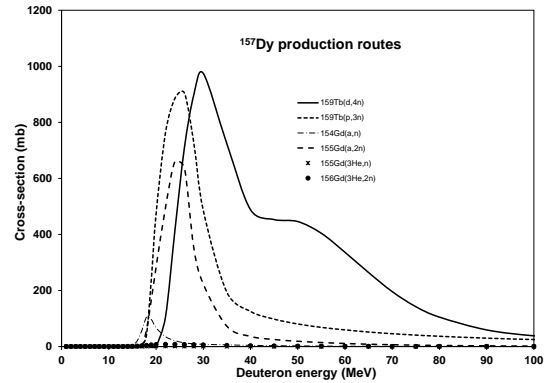


Figure 12: Comparison of excitation functions for production of  $^{157}\text{Dy}$



## References

- [1] A. Hermanne, F. Tárkányi, S. Takács, Production of medically relevant radionuclides with medium energy deuterons (2008).
- [2] F. Tárkányi, A. Hermanne, F. Ditrói, S. Takács, B. Király, G. Csikai, M. Baba, H. Yamazaki, M. S. Uddin, A. V. Ignatyuk, S. M. Qaim, Systematic study of activation cross-sections of deuteron induced reactions used in accelerator applications (25-28 Oct., 2010 2011).
- [3] F. Rosch, Radiolanthanides in endoradiotherapy: an overview, *Radiochimica Acta* 95 (6) (2007) 303–311.
- [4] M. Neves, A. Kling, A. Oliveira, Radionuclides used for therapy and suggestion for new candidates, *Journal of Radioanalytical and Nuclear Chemistry* 266 (3) (2005) 377–384.
- [5] H. Uusijarvi, P. Bernhardt, F. Rosch, H. R. Maেকে, E. Forsell-Aronsson, Electron- and positron-emitting radiolanthanides for therapy: Aspects of dosimetry and production, *Journal of Nuclear Medicine* 47 (5) (2006) 807–814.
- [6] D. Nayak, S. Lahiri, Application of radioisotopes in the field of nuclear medicine - i. lanthanide series elements, *Journal of Radioanalytical and Nuclear Chemistry* 242 (2) (1999) 423–432.
- [7] E. Lebowitz, M. W. Greene, The production of  $^{157}\text{Dy}$  for medical use, *The International journal of applied radiation and isotopes* 22 (12) (1971) 789–793.
- [8] D. Apo, Production of Dysprosium-157 from Proton Bombardment of Terbium-159, 1981.
- [9] Y. Yano, D. C. Van Dyke, J. Verdon, T. A., H. O. Anger, Cyclotron-produced  $^{157}\text{Dy}$  compared with  $^{18}\text{F}$  for bone scanning using the whole-body scanner and scintillation camera, *Journal of Nuclear Medicine* 12 (12) (1971) 815–21.
- [10] T. M. Duc, J. Tousset, Excitation function of reactions induced on terbium by 26.9 mev deuterons, *Comptes Rendus, Ser. A and B* 266 (1968) 100–102.
- [11] L. N. Siri, S. J. Nassiff, Excitation functions for  $^{159}\text{Tb}(d,p)^{160}\text{Tb}$  and  $^{159}\text{Tb}(d,n)^{157}\text{Dy}$  reactions, *Radiochimica Acta* 14 (1970) 159.
- [12] S. Mukhammedov, A. Vasidov, E. Pardaev, Use of proton and deuteron activation methods of analysis in the determination of elements with  $Z \leq 42$ , *Soviet Atomic Energy* 56 (1) (1984) 56–58.
- [13] A. Hermanne, R. Adam Rebeles, F. Tárkányi, S. Takács, M. P. Takács, A. Ignatyuk, M. S. Uddin, Excitation functions of deuteron induced reactions on natOs up to 50 mev: Experiments and comparison with theoretical codes, *Nuclear Instruments and Methods in Physics Research Section B: Beam Interactions with Materials and Atoms* 297 (0) (2013) 75–85.
- [14] F. Tárkányi, F. Ditrói, S. Takács, B. Király, A. Hermanne, M. Sonck, M. Baba, A. V. Ignatyuk, Investigation of activation cross-sections of deuteron induced nuclear reactions on natMo up to 50 mev, *Nuclear Instruments & Methods in Physics Research Section B-Beam Interactions with Materials and Atoms* 274 (2012) 1–25.
- [15] Canberra, [http://www.canberra.com/products/radiochemistry\\_lab/genie-2000-software.asp](http://www.canberra.com/products/radiochemistry_lab/genie-2000-software.asp).
- [16] G. Székely, Fgm - a flexible gamma-spectrum analysis program for a small computer, *Computer Physics Communications* 34 (3) (1985) 313–324.
- [17] F. Tárkányi, F. Szelecsényi, S. Takács, Determination of effective bombarding energies and fluxes using improved stacked-foil technique, *Acta Radiologica, Supplementum* 376 (1991) 72.
- [18] R. R. Kinsey, C. L. Dunford, J. K. Tuli, T. W. Burrows, *NUDAT 2.6, Vol. 2*, Springer Hungarica Ltd, Budapest, 1997, p. 657.
- [19] B. Pritychenko, A. Sonzogni, Q-value calculator (2003).
- [20] H. H. Andersen, J. F. Ziegler, Hydrogen stopping powers and ranges in all elements. *The Stopping and ranges of ions in matter*, Volume 3., The Stopping and ranges of ions in matter, Pergamon Press, New York, 1977.
- [21] I.-B. of-Weights-and Measures, Guide to the expression of uncertainty in measurement, 1st Edition, International Organization for Standardization, Geneva, Switzerland, 1993.
- [22] M. Bonardi, The contribution to nuclear data for biomedical radioisotope production from the milan cyclotron facility (1987).
- [23] F. Tárkányi, S. Takács, K. Gul, A. Hermanne, M. G. Mustafa, M. Nortier, P. Oblozinsky, S. M. Qaim, B. Scholten, Y. N. Shubin, Z. Youxiang, Beam monitor reactions (chapter 4). charged particle cross-section database for medical radioisotope production: diagnostic radioisotopes and monitor reactions., Tech. rep., IAEA (2001).
- [24] A. I. Dityuk, A. Y. Konobeyev, V. P. Lunev, Y. N. Shubin, New version of the advanced computer code alice-ippe, Tech. rep., IAEA (1998).
- [25] M. Herman, R. Capote, B. V. Carlson, P. Oblozinsky, M. Sin, A. Trkov, H. Wienke, V. Zerkin, Empire: Nuclear reaction model code system for data evaluation, *Nuclear Data Sheets* 108 (12) (2007) 2655–2715.
- [26] A. J. Koning, S. Hilaire, M. C. Duijvestijn, *Talys-1.0* (2007).
- [27] A. J. Koning, D. Rochman, *Talys-based evaluated nuclear data library version 4* (2011).
- [28] F. Tárkányi, A. Hermanne, S. Takács, K. Hilgers, S. F. Kovalev, A. V. Ignatyuk, S. M. Qaim, Study of the  $^{192}\text{Os}(d,2n)$  reaction for, production of the therapeutic radionuclide  $^{192}\text{Ir}$  in no-carrier added form, *Applied Radiation and Isotopes* 65 (11) (2007) 1215–1220.
- [29] A. Hermanne, F. Tárkányi, S. Takács, F. Ditrói, M. Baba, T. Ohtshuki, I. Spahn, A. V. Ignatyuk, Excitation functions for production of medically relevant radioisotopes in deuteron irradiations of pr and tm targets, *Nuclear Instruments & Methods in Physics Research Section B-Beam Interactions with Materials and Atoms* 267 (5) (2009) 727–736.
- [30] H. E. Hassan, F. S. Al-Saleh, K. F. Hassan, A. Sayed, Z. A. Saleh, Proton induced nuclear reactions on  $^{159}\text{Tb}$  and  $^{139}\text{La}$  for producing  $^{159}\text{Dy}$  and  $^{139}\text{Ce}$ , *Arab Journal of Nuclear Sciences and Applications* 43 (2010) 233–242.
- [31] D. V. Rao, G. F. Govelitz, K. S. R. Sastry, Dysprosium-159 for transmission imaging and bone mineral analysis, *Medical Physics* 4 (2) (1977) 109–114.
- [32] D. Habs, U. Koster, Production of medical radioisotopes with high specific activity in photonuclear reactions with gamma-beams of high intensity and large brilliance, *Applied Physics B-Lasers and Optics* 103 (2) (2011) 501–519.
- [33] G. J. Beyer, T. J. Ruth, The role of electromagnetic separators in the production of radiotracers for bio-medical research and nuclear medical application, *Nuclear Instruments & Methods in Physics Research Section B-Beam Interactions with Materials and Atoms* 204 (2003) 694–700.